JOURNAL OF GEOPHYSICAL RESEARCH, VOL. 105, NO. D6, PAGES 7103–7110, MARCH 27, 2000

Production of nitrogen oxides by a large spark generator

D. R. Cook, Y. P. Liaw, and D. L. Sisterson

Environmental Research Division, Argonne National Laboratory, Argonne, Illinois

N. L. Miller

Earth Sciences Division, Berkeley National Laboratory, University of California, Berkeley

Abstract. A large spark generator was used outdoors to determine the production of nitrogen oxides (NO_x) from sparks with characteristics similar to those of lightning strokes. The experiment was conducted at the Rocket Triggered Lightning Program facility at Cape Canaveral, Florida, in August 1991, during the Convection and Precipitation/Electrification field experiment. Plumes of NO_x from spark generations were sensed by a NO_x analyzer. The spark energy was $9.8 \pm 0.7 \times 10^4$ J, and the spark gap was 1.65 or 2.13 m. The plumes reached the analyzer inlet within 0.3–4.7 s after spark generation. The NO_x concentrations varied, depending on the geometry of the plume. Laboratory studies of analyzer response permitted adjustment of the measured concentrations to corrected concentrations. Production of NO_x, in terms of mass of nitrogen, averaged 22.5 ± 2.9 mg per spark, 11.7 ± 1.5 mg m^{-1} of spark length, and $1.1 \pm 0.2 \times 10^{16}$ molecules J^{-1}. The median ratio of nitric oxide (NO) to nitrogen dioxide (NO_2) was 0.76, indicating substantial conversion within a few seconds. Scaling of NO_x production to lightning energy levels and dimensions yielded an annual global NO_x production of 9.7 Tg yr^{-1}, similar to values estimated from recent thunderstorm measurements and modeling studies. Recent satellite measurements suggest that cloud-to-ground lightning flash frequency is an order of magnitude smaller than normally assumed; estimates of global NO_x production by lightning might also need to be reduced by an order of magnitude.

1. Background

In the past two decades, much effort has been spent in determining an estimate of the contribution of lightning to the atmospheric budget of nitrogen oxides (NO_x). To accomplish this, laboratory spark experiments, field experiments involving both natural and triggered lightning, and modeling studies have been performed. These have been reviewed by *Liaw et al.* [1990], *Lawrence et al.* [1994], *Lee et al.* [1997], and *Huntrieser et al.* [1998]. Some assumptions about lightning characteristics and frequency are used in scaling up measurements and modeling results to annual global levels of NO_x production. The normal assumptions are described by *Liaw et al.* [1990] and *Price et al.* [1997]. There is some controversy about the assumptions used, including global lightning flash frequency, the relative contribution of cloud-to-ground (CG) and intercloud and intracloud (IC) lightning, flash energy, and lightning stroke length. Global lightning flash frequency is normally assumed to be 100 s^{-1} [*Liaw et al.*, 1990], although satellite estimates suggest a range of 40–120 s^{-1} from Defense Meteorological Satellite Program (DMSP) satellites [*Turman and Edgar*, 1982] and the Ume-2 Ionospheric Sounding Satellite (ISS-b) [*Kotaki and Katoh*, 1983], and more recently, 36.8 s^{-1} from the optical transient detector (OTD) [*Christian et al.*, 1999]. The same NO_x production level is assumed for each flash, even though IC flashes (which are about one tenth as energetic as CG flashes) appear to account for 66–75% of all flashes [*Price et al.*, 1997]. CG flash energy has typically been assumed to be 4×10^8 J [*Borucki and Chameides*, 1984] to 6.7×10^9 J [*Price et al.*, 1997].

Despite the controversy over scale-up assumptions used, the NO_x production by a typical lightning flash is the greatest unknown that remains [*Price et al.*, 1997]. The measurement of NO_x concentration immediately after a spark discharge, in a more controlled setting than during a thunderstorm, has been the goal of a number of investigators. Laboratory spark studies conducted by *Chameides et al.* [1977], *Levine et al.* [1981], *Peyrous and Lapeyre* [1982], *Hill et al.* [1988], and *Wang et al.* [1998] produced a wide range of results, which when normalized to the standard set of assumptions of *Liaw et al.* [1990] yield annual global NO_x production values of 5.2–30 Tg yr^{-1}. Recent measurements from thunderstorms fall near the bottom of this range, and modeling studies yield values in the bottom half of this range.

2. Methods and Observations

2.1. Experiment Design

We designed an experiment to measure the NO_x production from large spark generations in an outdoor setting, as opposed to a laboratory setting. In August 1991, in conjunction with the CAPE (Convection and Precipitation/Electrification) field experiment, we used a modified oxides-of-nitrogen analyzer to measure the production of NO_x from sparks generated with the Boeing Aerospace Corporation HGV-8 lightning simulator outdoors at the Rocket Triggered Lightning Program (RTLP) facility at Cape Canaveral, Florida. This large spark generator produced sparks with a peak current similar to lightning first

Paper number 1999JD901138.
0148-0227/00/1999JD901138$09.00

strokes. The Boeing lightning simulator had been used primarily by the U.S. Navy to simulate and assess lightning damage to aircraft and ship components. Our goal in using a large spark generator outdoors was to obtain NO_x production by integrating the measured NO_x concentration over the observed portion of the plume. Knowing the spark characteristics with precision, we translate the observed NO_x concentrations into annual global production terms by using scaling techniques reported in the literature. We then compare our results with those obtained from other spark studies, recent thunderstorm measurements of NO_x, and recent modeling studies.

2.2. Lightning Simulator

The HGV-8 Lightning Simulator is a 4.7 Mv, Marx-type impulse generator, with the charging/firing electrical circuit contained in a semitrailer. An elevated cable carries the generator energy to a discharge point, suspended a few meters above the sandy soil, and the return electric flow is provided by flat-braided grounding cables running back along the sand from the base point, a meter above the sand, to the semitrailer. Two columns of 22 pairs of 0.4 microfarad and 16 pairs of 0.25 microfarad capacitors (152 capacitors total) were used in the charging circuit to reduce series inductance. A 2 kilohm wire-wound resistor for each pair of capacitors permits each of the 76 pairs of capacitors to be charged to 62 kv. Each capacitor-resistor set is grounded to the semitrailer frame, allowing the semitrailer and enclosed electrical system to float. The system is not critically damped. The capacitor columns are charged in series but are discharged in parallel to produce a virtually continuous current that is approximated by the calculated peak current. Capacitor pairs are separated by open air gaps set at precisely the right distance to "hold off" the potential between capacitor pairs until a discharge is initiated to the first three open air gaps of each column of capacitors by a small trigger generator. The breakdown of subsequent gaps is nearly simultaneous, with a total discharge time of 47 μs. The discharge process was controlled from an electronic panel housed in a step van located 30 m from the discharge points. The generator efficiency is estimated at 93–97% by the engineers who designed the system. These and other details of the HGV-8 lightning simulator are found in a report to NASA by P. Medelius and A. Eckoff (Simulated lightning and measurement systems on the space shuttle payload changeout room, I-NET, Inc., Dec. 1993).

The total output voltage (4.7 Mv) to the spark discharge points is the summation of the capacitor charge voltages. The spark generations yielded a discharge electric field of 2.4×10^6 v m^{-1}, a peak current of 36 kA, a spark energy of 98.4 kJ, and thus a spark energy per gap length of 49.2 kJ m^{-1} for a spark gap of 2 m [*Medelius and Eckoff*, 1993]. These figures can be compared with the mean characteristics of a typical, natural, lightning first return stroke over land: 5×10^4 v m^{-1} [*Winn et al.*, 1974], 30.2 kA [*Wacker and Orville*, 1999] to 35.7 kA [*Price et al.*, 1997], and approximately 800 kJ m^{-1} (for a 7 km stroke) [*Liaw et al.*, 1990; *Price et al.*, 1997].

2.3. Air Quality and Meteorological Measurements

Concentrations of NO and NO_x were measured with a Thermo Electron Corporation (TECO) 14D/E oxides-of-nitrogen analyzer. Ozone (O_3) concentration was measured with a Dasibi 1003-AH fluorescence O_3 analyzer. The analyzers were located several meters from the spark gap and were equipped with Teflon sampling tubes of 3 m length and 0.33 cm outside diameter with small Teflon filters at the inlets. The tubes were extended along wood poles with the inlet filters placed at the midheight of the spark gap and 3.7–5.5 m horizontally away. We located the inlet filters downwind of the spark gap. The actual wind direction determined whether a spark plume was observed, and if so, what portion was observed.

The TECO oxides-of-nitrogen analyzer had been modified to a fast-response sensor by altering the electronic filtering to give an electronic response time of 0.5 s. A design advantage of the TECO analyzer is a split reaction chamber which allows continuous measurement of both NO and NO_x. The Dasibi 1003-AH fluorescence O_3 analyzer provided background O_3 concentrations; the analyzer has a minimum 12 s integration time and therefore was not sufficiently capable of resolving O_3 concentrations in the spark plumes.

A meteorological monitoring system was installed 5 m west of the spark gap to provide measurements of wind speed, wind direction, temperature, and humidity. Meteorological measurements were averaged to 1 min values by a Campbell Scientific, Inc. CR21X data logger.

Faraday cages were fashioned from lumber and fine-mesh metal screening to shield the air quality analyzers and data acquisition equipment from the effects of induced voltage produced by the large electric field of the spark discharge. All power and data cables to the instruments were shielded inside copper braid, and the cages, copper braid, and meteorological sensor mount were grounded. The largest Faraday cage housed a laptop computer used to monitor and download data from Campbell Scientific, Inc. CR21X dataloggers, a strip chart recorder to record the signals from the TECO analyzer, and the operator of the equipment. One datalogger recorded the meteorological information, while the other recorded ozone and oxides-of-nitrogen analyzer outputs at a 1 Hz rate. The strip chart recorder (0.5 s response time) provided continuous information from the TECO oxides-of-nitrogen analyzer. The Faraday cages and grounding system reduced electric field effects from the spark generations to a small electronic spike on the strip chart recorder at the time of discharge. The electronic spike occurred for each spark discharge (thereby serving as an excellent marker for the discharge time), whether NO_x was sensed by the analyzer or not, was very distinct, exhibited rapid recovery indicating that the effect was purely electronic in nature, and occurred so much before NO_x was sensed, that NO_x concentration measurements were not considered to be contaminated.

2.4. General Observations

The meteorological measurements (1 min averages) showed that the atmospheric conditions under which the spark generation observations took place were similar each day, with a wind speed of less than 3 m s^{-1}, partly cloudy sky, 75–80% relative humidity, and 35°–38°C temperature. Average wind directions were east to southeast on August 7 and 8, 1991, and west to northwest on August 9, 1991. The short distance from the spark gap to the analyzer inlets allowed little time for dispersion of the plume by atmospheric turbulence. The leading edge of the plume reached the TECO analyzer inlet within a few seconds after spark generation, although the time interval varied, depending on wind speed, wind direction, and plume width. Ambient O_3 concentrations were 35–45 ppbv, and ambient NO_x concentrations were less than 5 ppbv during each of the three measurement days.

A magnitude range of NO_x concentrations was observed as a consequence of the variation of the width and angle of approach of the plumes to the analyzer inlets. The locations of the discharge points and the oxides-of-nitrogen analyzer inlet were changed, so the analyzer inlet was downwind of the spark generation. Plumes from 20 sparks were observed over a 3-day period by using spark gaps of 1.65, 2.13, and 2.26 m. Of the 20 spark plumes observed by the TECO oxides-of-nitrogen analyzer during the three days of the experiment, 14 plumes were included in our final data set, based on the following criteria: the plume must arrive at the analyzer inlet within 5 s and the calculated plume radius must be within approximately one standard deviation of the average for the plumes observed that day. Seven of the eight plumes on August 7, none of the three plumes on August 8, and seven of the nine plumes on August 9 met our selection criteria. The average NO_x concentration of the 14 plumes that met the criteria was more than 5 times that of the average for the other six plumes. The entire, or nearly entire, width of the plume was considered to have been observed during the 14 accepted cases.

Although axial expansion of the plume probably occurred, it was probably small compared to the radial expansion. We did not consider axial expansion in calculations of NO_x production by the spark; therefore the NO_x production may be underestimated.

An average NO_x concentration of 1367 ppbv was observed in plumes from the 14 spark generations, in contrast to the ambient NO_x concentration of 5 ppbv; this is equivalent to 1.1×10^{21} molecules per spark and 1.1×10^{16} molecules J^{-1}. Since the 1 Hz sampling rate of the CR21X datalogger was not fast enough to reliably capture the peak NO_x concentration in the spark plume, peak concentrations were determined from the strip chart record of the analyzer output, as described below.

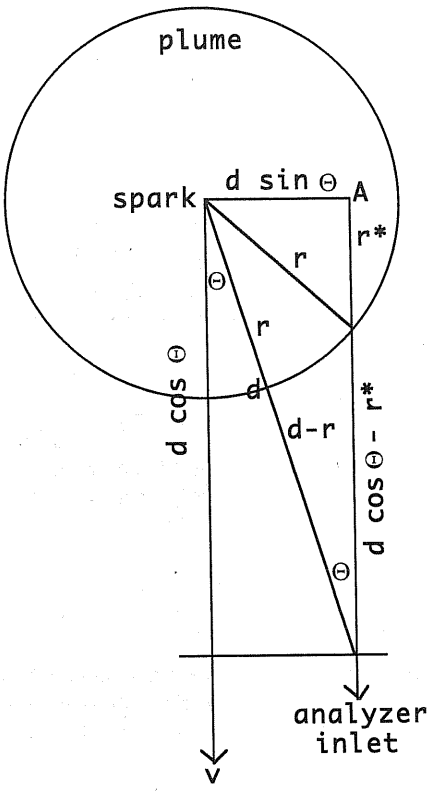

Figure 1. Geometry of the angle of incidence of the spark plume to the oxides-of-nitrogen analyzer inlet.

3. Data Analyses

3.1. Adjustments To Measurements

Adjustments to the strip chart record of NO_x measurements for frequency response of the TECO 14D/E oxides-of-nitrogen analyzer were required to obtain corrected NO_x concentrations. The analyzer and strip chart response times caused a reduction of recorded NO_x voltage output. Therefore the integrated area under the strip chart curve of the analyzer output is not exactly proportional to NO_x concentration, nor is the width of the plume record on the chart an accurate indicator of exposure time (t_e) to the plume. The analyzer was not capable of responding fully to the large NO_x concentration encountered over the order of seconds, nor was the response sufficient to detect concentration variations in the plume. The area under the strip chart curve is therefore somewhat smoothed. The time required for the strip chart to reach a peak (ttp) from the plume is directly proportional to t_e and to the average plume NO_x concentration. This was confirmed in 62 laboratory trials performed at three concentration levels (100, 200, and 400 ppbv) of NO and NO_2 for both the NO and the NO_x channels of the TECO. The relationship between ttp and t_e and appropriate adjustments to measured NO and NO_x concentrations were determined from these studies. The details of the studies and adjustments determined are described in Appendix A.

3.2. Determination of Plume Widths

Meteorological measurements were combined with measurements of t_e to determine spark plume trajectory, allowing calculation of the spark plume radius at the time of arrival at the TECO analyzer inlet. Wind direction measurements indicated that the center of the spark plume did not always pass through the position of the analyzer inlet. Furthermore, plume width varied with the length of time after spark generation and the spark gap used. Figure 1 shows the geometry used in calculating the plume radius. Details of the technique are found in Appendix B.

In the short period between spark generation and the observation of NO_x by the analyzer, expansion of the spark plume is determined principally by the dissipation of energy in the spark channel. Although the same energy was used for each spark generation, the spark gap was different for each day of observations, resulting in different amounts of energy per meter of spark channel (29% greater for the shortest than for the longest gap) and therefore different plume radii, plume volumes, and NO_x concentrations. This observation can be seen in a comparison of the average of those three quantities for the two gaps used: 2.0 m, 26.8 m^3, and 575 ppbv (2.13 m gap) versus 3.3 m, 56.4 m^3, and 1931 ppbv (1.65 m gap), respectively. Greater energy per gap length resulted in larger plume radii and larger NO_x concentrations.

The spark plume radius shortly after spark generation can be predicted with a channel expansion model. A model by *Hill* [1990] predicts that virtually all of the heat-induced expansion occurs in the first 200 ms and that the resulting plume radius is proportional to the amount of input energy. *Hill* [1990] used nondimensional representations of plume radius (R) and time (τ) to illustrate the results of channel expansion modeling work by different investigators. We fitted a power law curve through the data points of *Hill* [1990] and *Plooster* [1971], as well as a

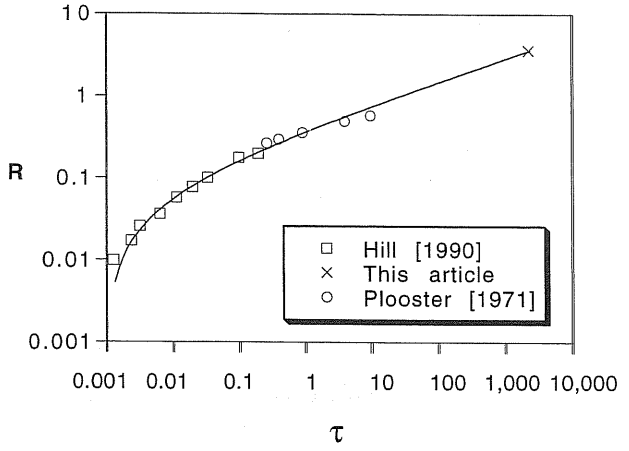

Figure 2. Power curve calculated from equation (1), plotted over data points from *Hill* [1990] (squares), *Plooster* [1971] (circles), and our average data value (cross).

point representing the average of our results. Channel radius can then be estimated for various time intervals. The curve fits the data quite well for τ greater than 0.002 and is represented by

$$R = -0.06 + 0.42\tau^{0.28}. \quad (1)$$

The data and curve are plotted in Figure 2. Equation (1) produces R of 0.2 for τ of 0.2, in agreement with *Hill* [1990] who suggested that these are the appropriate values at the equilibrium pressure temperature of 11,000 K. A discussion of the agreement of (1) with modeled radii found by other investigators is in Appendix C.

At 100 ms after the spark, (1) predicts a radius of 75 cm for our spark channel. By this time, atmospheric dispersion might have begun to contribute to channel expansion. However, Figure 2 suggests that heat expansion might still be dominant more than 1 s after the spark discharge. This finding is consistent with an early channel expansion model of *Hill et al.* [1980], which indicates that ambient temperature is not reached in the channel until at least 1 s has passed, if a moderate mixing ratio of 10 cm^3 s^{-1} is assumed. The data of *Hill* [1990, Figure 3] also suggest that ambient temperature is reached at about 1 s. Our data indicate larger radii than the *Hill* [1990] expansion model predicts after 1 s. This might be partially explained by the slightly longer duration of spark discharge (47 us), in comparison to that of a typical lightning stroke (30 us) (H. J. Christian and M. A. McCook, A lightning primer, p. 2, Characteristics of a storm: Lightning, available at http://thunder.msfc.nasa.gov/primer/primer2.html, 1999), and by the effects of atmospheric dispersion.

The atmospheric dispersion equation (11) in Appendix B predicts that a 0.75 m initial plume radius (1 s after discharge) increases by no more than 20% for any of the spark observations, with a minimum increase of 6%. Because atmospheric dispersion is very small over the short times of the observations, heat expansion of the spark channel apparently continued for longer than has been predicted by lightning channel models. Equation (1) adequately represents plume expansion for our spark observations in the first few seconds after the spark discharge.

4. Nitrogen Oxides Production Calculations

We assume that our measurements of NO_x concentration represent the average concentration in the spark plume in the first few seconds after the spark discharge. We calculate the production of nitrogen oxides, Q_p, from

$$Q_p = CV, \quad (2)$$

where C is NO_x density in g cm^{-3} and V is the volume of the spark plume in cm^3. The production from 14 spark discharges averaged 22.5 ± 2.9 mg, with a maximum value of 77.1 mg, a minimum value of 8.9 mg, and a median value of 18.1 mg. This translates to a production per unit spark length of 11.7 ± 1.5 mg m^{-1}, more than an order of magnitude smaller than a value of 320 mg m^{-1} found by *Holler et al.* [1999] in natural lightning. This result was expected because of the lower energy of the spark ($9.8 \pm 0.7 \times 10^4$ J or 4.9×10^4 J m^{-1}) in comparison with that of a typical lightning stroke (5–6.7 $\times$ 10^9 J or ~800 kJ m^{-1} for a 7 km stroke) [*Liaw et al.*, 1990; *Price et al.*, 1997].

The average production of NO molecules by the 14 spark discharges (assuming that all measured NO_x was NO originally) was 1.1 ± $\times$ 10^{16} molecules J^{-1}, comparable to the results of laboratory spark discharge studies (all figures $\times$ 10^{16} molecules of NO J^{-1}): 1.4 for a 5.7×10^{-3} J spark by *Hill et al.* [1988], 5 for a 1.2×10^4 J spark by *Levine et al.* [1981], 6 for a 3.6×10^{-2} J spark by *Chameides et al.* [1977], 8 for a 1.35×10^3 J spark by *Chameides et al.* [1977], and an average of about 30 for an unknown spark energy by *Wang et al.* [1998].

Our results can be further compared with data from previous spark tests, model estimates, and thunderstorm measurements by scaling them up to CG lightning flash energy. To estimate annual global NO_x production, we use a global flash rate of 100 s^{-1}, a minimum flash energy of 4×10^8 Joules [*Borucki and Chameides*, 1984] and a maximum flash energy of 6.7×10^9 Joules [*Price et al.*, 1997], and a doubling of the spark production (to 45 mg per spark) to scale up from a single spark stroke to multiple strokes (as in a lightning flash) and to include IC flash production as done by *Liaw et al.* [1990]. The result is

$$G = Q_p(3.15 \times 10^7 \text{ s yr}^{-1})(100 \text{ s}^{-1})(\text{flash energy})(9.8 \times 10^4 \text{ J})^{-1}, \quad (3)$$

where Q_p is in grams, the last two terms form the ratio of lightning energy to spark energy, and G is in units of grams per year. Equation (3) yields values of 0.6 and 9.7 Tg yr^{-1} (for minimum and maximum flash energies, respectively) for our spark data. These results are comparable to values estimated from recent model studies (5 Tg yr^{-1} by *Lee et al.* [1997] and 12.2 Tg yr^{-1} by *Price et al.* [1997]), bracket the range of values estimated from thunderstorm measurements of NO_x production recently quoted in the literature (2 Tg yr^{-1} [*Lawrence et al.*, 1994]; 2–6 Tg yr^{-1} [*Levy et al.*, 1996] and [*Ridley et al.*, 1996]; 4 Tg yr^{-1} [*Huntrieser et al.*, 1998]; 5 Tg yr^{-1} [*Holler et al.*, 1999]), and fall in the lower half of the range of values estimated from laboratory spark studies (22–30 Tg yr^{-1} [*Chameides et al.*, 1977]; 18.5 Tg yr^{-1} [*Levine et al.*, 1981]; 5.9 Tg yr^{-1} [*Peyrous and Lepeyne*, 1982]; 5.2 Tg yr^{-1} [*Hill et al.*, 1988]; 8.3 Tg yr^{-1} [*Wang et al.*, 1998]). Flash energies and lightning channel length are not given in most of the thunderstorm measurements papers. However, information available from *Ridley et al.* [1996] indicates that the lightning channel lengths were less than 8 km. *Holler et al.* [1999] assumed a channel length of 5

km; 7 Tg yr^{-1} would result from a 7 km channel, as we assume. From *Wang et al.* [1998], a flash energy of 4×10^7 J can be derived for a 7 km flash; this flash energy is at least an order of magnitude smaller than the value accepted for lightning flash energy. *Price et al.* [1997] assume a large flash energy of 6.7×10^9 J per flash, but a low flash frequency of 30 per second; using the common assumption of 100 s^{-1} for flash frequency yields a production of 40.7 Tg yr^{-1} for their data.

For the spark for which we obtained the largest NO_x production, estimates of global annual production of 2.1 Tg yr^{-1} would result for the minimum flash energy of 4×10^8 J and 35.2 Tg yr^{-1} for the maximum flash energy of 6.7×10^9 J. These values also fall within the magnitude size range (2–40 Tg yr^{-1}) of global annual production estimated from the thunderstorm measurements, spark studies, and modeling studies mentioned above. We believe that the most representative global annual production value for our results is 9.7 Tg yr^{-1}, based on our average measured NO_x density and a flash energy of 6.7×10^9 Joules [*Price et al.*, 1997]. It may be important to note that although we did so for our results, not all of the production values obtained by the authors quoted above may include an adjustment for the production of NO_x by IC flashes; therefore some of those values may be underestimates. In fact, our value of 9.7 Tg yr^{-1} may be a slight underestimate because we did not consider axial expansion of the spark plume and because we did not sample the entire width of all of the plumes.

5. Discussion of Results

5.1. Global Production Estimates

The annual global production estimates made by the various investigators quoted above may need to be adjusted downward, on the basis of recent measurements of global lightning flash frequency by the OTD satellite. OTD measurements suggest a global flash frequency of about 37 s^{-1} [*Christian et al.*, 1999]. If the OTD satellite instrument is equally capable of detecting IC and CG flashes and IC flashes are 3 to 5 times as frequent as CG flashes [*Liaw et al.*, 1990; *Mackerras et al.*, 1998], the OTD measurements would indicate a global CG frequency of the order of 10 s^{-1}. This possibility was also alluded to by *Mackerras et al.* [1998], based on measurements of the latitudinal variation of CG flashes. This estimate of global CG frequency is an order of magnitude smaller than the 100 s^{-1} value normally assumed in the calculations of annual global NO_x production estimates.

Therefore previous estimates of annual global NO_x production might be an order of magnitude too large. Adjusting production estimates to account for this new information would reduce the likely range of annual global NO_x production to 0.2–4 Tg yr^{-1}. This range may still be overestimated, when considering that 75% of flashes occur between 30° north and 30° south latitudes, with the IC:CG ratio tending to be larger in the tropics than in the temperate areas (where most of the NO_x production measurements have been made).

Another issue that is not usually addressed in the calculation of estimates of annual global NO_x production is that surface-based measurements (laboratory and outdoor spark tests) may produce overestimates because they do not make adjustments for the likely decrease in production in a lightning channel with increasing altitude [*Goldenbaum and Dickerson*, 1993].

5.2. Spark Plume Chemistry

The median ratio of NO to NO_2 in the spark plumes was 0.76. For 62% of the plumes, NO_2 exceeded NO, and for 69%, the ratio was less than 2, suggesting rapid conversion of NO to NO_2 after spark generation. Substantial conversion from NO to NO_2 apparently occurs within a few seconds. The reaction $NO + O_3 \rightarrow NO_2 + O_2$ is often quoted as the one by which the conversion takes place, but the availability of ambient and plume O_3 is too small, and the mixing of these into the spark plume is too slow [*Franzblau and Popp*, 1989] to account for the conversion rate observed in our data. The concentration of O_3 produced by lightning is lower by 2 [*Hill et al.*, 1980] to 4 [*Tuck*, 1976] orders of magnitude than the concentration of NO produced and therefore is not a significant contribution to the conversion process.

The increase in chemical reaction rates by elevated temperatures (those occurring in a lightning channel above ambient temperature to approximately 1000 K) should be considered as a mechanism to explain the rapid conversion of NO to NO_2 in the spark plume. Ionization and chemical reaction rates are highly electron temperature dependent, affecting transfer of energy among species, radiation emission and absorption, and energy dissipation [*Goldenbaum and Dickerson*, 1993]. Three potentially important reactions are listed below with reference(s), the reaction rate k, the temperature T at which the rate was determined, and the production rate p of NO_2. The production rates were determined by using ambient concentrations of the constituents (for example, O_3 at 35 ppbv), with the exception of NO concentration in the plume at 2000 ppbv (similar to what we measured) and monatomic oxygen as 0.02% of O_2. Monatomic oxygen might be underestimated, as the amount of O_2 dissociated into O by the spark is not known. The three potentially important reactions are as follows: (1) $NO + O_2 \rightarrow NO_2 + O$ [*Bemand et al.*, 1973; *Baulch et al.*, 1973] $k = 5 \times 10^{-12}$ cm^3 $molecule^{-1}$ s^{-1}, $T = 1000$ K, $p = 1.3 \times 10^{21}$ molecules cm^{-3} s^{-1}; (2) $NO + O + M \rightarrow NO_2 + M$, where M is a third body such as nitrogen, argon, or oxygen; for N_2 [*Kaufman et al.*, 1956] $k = 1.7 \times 10^{-32}$ cm^6 $molecules^{-2}$ s^{-1}, $T = 900$ K, $p = 8.5 \times 10^{16}$ molecules cm^{-3} s^{-1}; for Ar [*Yarwood et al.*, 1991] $k = 3.3 \times 10^{-32}$ cm^6 $molecules^{-2}$ s^{-1}, $T = 500$ K, $p = 1.9 \times 10^{15}$ molecules cm^{-3} s^{-1} for O_2 production; the reaction rate falls between those for N_2 and Ar; (3) $NO + O \rightarrow NO_2$ [*Baulch et al.*, 1973] $k = 6.6 \times 10^{-8}$ cm^3 $molecule^{-1}$ s^{-1}, $T = 1{,}000$ K, $p = 1.7 \times 10^{22}$ molecules cm^{-3} s^{-1}.

Each of these reactions is several orders of magnitude faster, at elevated temperatures, than the $NO + O_3$ reaction at ambient temperature ($k = 2 \times 10^{-4}$ cm^3 $molecule^{-1}$ s^{-1}; $T = 300$ K; $p = 9 \times 10^{11}$ molecules cm^{-3} s^{-1}; rate coefficient from *Michael et al.* [1981]). Two of the three reactions are dependent on the availability of monatomic oxygen. Those two reactions could contribute to the concentrations of NO_2 that we observed if significant amounts of monatomic oxygen are liberated from O_2 by lightning energy, as suggested by *Hill et al.* [1980]. The production of NO_2 by the reactions above is considerably offset, above 1000 K, by the thermal decomposition of NO_2 [*Yarwood et al.*, 1991]. Therefore most NO_2 production would occur below 1000 K. Other NO to NO_2 reactions have been recognized as being too slow to be of importance in NO_2 recombination. An example is the three-body reaction $NO + NO + O_2 \rightarrow NO_2 + NO_2$ [*Ford and Endow*, 1957] (production rate of 10^8 molecules cm^{-3} s^{-1}).

6. Conclusions

Use of a large spark generator enabled us to measure the production of NO_x by sparks with characteristics similar to those of lightning strokes. Production of NO_x, in terms of mass of nitrogen, averaged 22.5 mg per spark, 11.7 mg per meter of spark length, and 1.1×10^{16} molecules J^{-1}. The production results are consistent with laboratory spark studies. The measured ratios of NO to NO_2 in the spark plumes (median = 0.76) infer that conversion of NO to NO_2 was rapid, with typically one half of the NO having been converted within a few seconds. A mechanism to explain this rapid conversion might be found in the following reactions at elevated temperatures: $NO + O_2 \rightarrow NO_2 + O$; $NO + O + M \rightarrow NO_2 + M$; and $NO + O \rightarrow NO_2$. These reactions are several orders of magnitude faster than the $NO + O_3$ reaction, for which the availability of ambient and plume O_3 is insufficient for it to be important.

Because our measurements were performed outdoors, in Florida, in midsummer, our NO_x production results might be most applicable for subtropical areas. Our NO_x production results were scaled up to lightning energy levels and dimensions by using common assumptions for lightning characteristics quoted in the literature. The scale-up yields an estimate of annual global NO_x production of 9.7 Tg yr^{-1} of nitrogen, which falls above the range of recent estimates from thunderstorm measurements (2–6 Tg yr^{-1} of nitrogen) and within the ranges of recent modeling studies (5–12 Tg yr^{-1} of nitrogen) and laboratory spark studies (5–30 Tg yr^{-1} of nitrogen), as discussed in section 4. Surface-based measurements (laboratory and outdoor spark tests) may produce slight overestimates of the annual global NO_x production because they do not make adjustments for the likely decrease in production in a lightning channel with increasing altitude [*Goldenbaum and Dickerson*, 1993]. Furthermore, the most recent satellite measurements suggest that global CG lightning flash frequency is an order of magnitude smaller than the normally assumed value of 100 s^{-1}. Therefore recent estimates of annual global NO_x production by lightning might also need to be reduced by an order of magnitude, to 0.2–4 Tg yr^{-1}. Satellite measurements using improved sensors, such as the lightning imaging sensor (LIS) on the Tropical Rainfall Measuring Mission (TRMM) satellite launched in late 1997, promise to reduce this uncertainty.

Appendix A: NO_x Concentrations Determined From Response Time Considerations

The strip chart recorder used in the laboratory trials was the same the one used in the field experiment. Exposure times of 1–11 s were produced by switching a calibration gas flow in and out of ambient air. One part per billion by volume or less of NO_x was measured in the laboratory ambient air. The strip chart records were analyzed to determine relationships (4) through (7). The actual exposure time t_e is related to ttp as follows:

$$NO_x \text{ channel } t_e = -1.36 + 1.13 \text{ ttp}, \quad (4)$$

$$NO \text{ channel } t_e = -1.35 + 1.14 \text{ ttp}, \quad (5)$$

where t_e is actual exposure time in seconds, and ttp is the time required to reach the concentration peak in seconds. The linear correlation coefficient is 0.99 for both (4), with 41 data points, and (5), with 20 data points. Note that (4) and (5) are virtually the same, indicating the similar response of the NO and NO_x channels. Furthermore, because the NO_x channel had greater sensitivity and produced a larger, and thus more easily readable, strip chart deflection, the values of t_e obtained from the NO_x channel field measurements are used in analyses of the field observations.

The adjusted concentrations of NO_x from the strip chart record were determined as follows:

$$\text{adjusted } NO_x = 186 - 29.24 \text{ ttp} + 1.764 \text{ } NO_x, \quad (6)$$

$$\text{adjusted NO} = 209 - 28.98 \text{ ttp} + 2.081 \text{ NO}, \quad (7)$$

where NO_x and NO are the concentrations reflected by the strip chart deflections. Plumbing losses in the TECO 14D/E oxides-of-nitrogen analyzer were only 1–3 ppbv.

Appendix B: Estimating Atmospheric Dispersion of Spark Plumes

The dimension r^* is half of the portion of the plume detected by the TECO 14D/E oxides-of-nitrogen analyzer and is calculated from

$$r^* = 0.5 v t_e, \quad (8)$$

where v is wind speed in m s^{-1}. The angle Θ, determined from measured wind direction, enables us to calculate v from

$$v = (d \cos \Theta) tt^{-1}, \quad (9)$$

where d is the distance from the spark gap location to the analyzer inlet, and tt is the total time required for a point A (see Figure 1) in the plume to move to the analyzer inlet location.

The time interval between the spark generation and the earliest sensing of the plume by the analyzer is easy to determine from the strip chart record. Despite the shielding of the analyzer and the power and signal cables, the strong electromagnetic field of the spark generation caused a small electronic spike on the strip chart record. In the field the spike was observed to occur precisely at the spark time. The arrival time of the NO_x signal at the analyzer reaction chamber was clearly indicated by a sudden, rapid increase and then recovery in the strip chart recording. After the peak concentration was reached, the strip chart record dropped sharply at first, then more slowly as the analyzer flushed the large concentration from its plumbing. The interval between the electronic spike and the time the plume was sensed and recorded is related to the time required for the plume to be blown by the wind from the spark gap to the analyzer inlet and transported through the sample tube to the analyzer. The analyzer sampling delay, a function of the plumbing volume and pumping speed, must be removed from this interval to obtain the desired time interval. A storage oscilloscope was used in the laboratory to determine the delay time, in conjunction with the use of a small NO concentration. The delay time was measured as 2 s for both the NO and the NO_x channels of the TECO analyzer, using the inlet tube and filter employed during spark experiments. The radius r of the dispersed plume is determined with geometry (see Figure 1) as

$$r = [(r^*)^2 + (d \sin \Theta)^2]^{0.5}, \quad (10)$$

where $d \sin \Theta$ is the radial distance from the plume center to the outermost point of the plume detected by the analyzer.

Table 1. Spark and Lightning Channel Characteristics

Reference	Energy, 10^4 J m^{-1}	Channel Characteristics			
		11,000 K		3,000 K	
		Radius, cm	Time, ms	Radius, cm	Time, ms
Picone et al. [1981]	1.0	5.4	0.16	6.0	0.19
Hill [1990]	1.5	6.6	0.19	9.3	0.44
This article	4.7	12.0	0.35	16.8	0.81
Lightning stroke	32.9	30.7	0.89	43.0	2.08

To check the accuracy of the calculated radii, we compare them with an estimate of plume radius determined from a similarity formula applied to puff diffusion [*Hanna et al.*, 1982]. On the basis of (1) we assume that heat expansion from the spark generation results in an approximate radius r_o of 0.75 m within 100 ms. For the assumption that further expansion results from atmospheric dispersion, the plume radius r_p, in meters, can be estimated from

$$r_p = 0.5[4r_o + \mathrm{ctt}^2\,(2\varepsilon r_o)^{0.67}]^{0.5}, \qquad (11)$$

where ε is the eddy dissipation rate, which is primarily a function of atmospheric turbulence intensity, and c is a coefficient that we approximate to be 1 for our application. For atmospherically unstable conditions, ε is approximated by $1.8u^{*3}/z$, where z is spark gap midheight, and u^* is the friction velocity (approximately one tenth of the wind speed); the constant 1.8 was determined by *Frenzen and Vogel* [1992].

Appendix C: Estimating Plume Radius with Model Equations

Estimates of channel radius and time calculated with (1) and the nondimensional relationships 1 and 2 of *Hill* [1990] were made from the spark data of *Hill* [1990], a lightning stroke estimate of *Picone et al.* [1981], our spark data, and a commonly assumed lightning stroke energy per unit length [*Liaw et al.*, 1990]. The lightning stroke energy of *Picone et al.* [1981] is smaller by more than an order of magnitude than the energy of a typical CG stroke. Table 1 shows that channel radius, channel volume, and time of cooling are proportional to energy per unit length. Although our sparks had 3 times the energy of the *Hill* [1990] spark, (1) predicts that our spark channel would have a radius approximately twice that obtained by *Hill* [1990] at the time of pressure equilibrium (11,000 K). Because nearly all of the energy is dissipated via expansion of the channel, the channel volume is more nearly linearly in proportion to energy input than to radius. All of the calculated radii and times for 11,000 K are based on an R value of 0.2 and a τ value of 0.2. A typical lightning stroke channel might have a radius of as large as 30 cm at this point.

Equation (1) yields consistent results for the different data sets when the energy per unit volume of the channel is considered. At the pressure equilibrium temperature, *Hill* [1990] found his channel to have an energy per volume of 0.73 J cm^{-3}, whereas the same quantity for *Picone et al.* [1981] is 1.09 J cm^{-3}, for our sparks is an average of 1.04 J cm^{-3}, and for the typical lightning stroke is 1.11 J cm^{-3}. These values are consistent with a statement by *Picone et al.* [1981] that the value should be ~1 at the pressure equilibrium temperature.

The radii for 3000 K listed in Table 1 for *Hill* [1990] and *Picone et al.* [1981] are as quoted in their articles. At this temperature, where recombination chemistry begins, our spark channel is predicted by (1) to have a radius that is not quite twice that and a volume that is ~3 times that of *Hill* [1990]. Again, these results seem reasonable, considering the large difference in input energy. Because the nondimensional R and τ are basically ratios incorporating the consequences of the energy input, they should be approximately the same for all energy inputs at a particular temperature of the channel. The data of *Picone et al.* [1981] imply little plume growth after the pressure equilibrium time is reached, resulting in what appears to be an unrealistically small difference in radii between 11,000 and 3000 K. Although the channel might begin to be subject to expansion via atmospheric dispersion at 3000 K, the channel energy per volume should still be fairly consistent for different energy inputs. At this temperature the information in Table 1 yields energy per volume values of 0.88 J cm^{-3} for *Picone et al.* [1981], 0.55 J cm^{-3} for *Hill* [1990], 0.53 J cm^{-3} for the average of our sparks, and 0.57 J cm^{-3} for a typical lightning stroke. Because the channel volume and energy of *Picone et al.* [1981] suggest that their radius is underestimated, the larger energy per unit volume is expected. The lightning stroke radius at 3000 K is 43.0 cm and the time is 2.08 ms; the time period is smaller by more than an order of magnitude than the 50 ms suggested by *Uman and Voshall* [1968] in their early work.

Appendix D: Uncertainty Analysis Performed for Equation (10)

The spark generator results contain some uncertainties, due primarily to the limitations of the wind direction information available and corrections to the measured NO_x concentrations. The main contribution to the uncertainty in Q_p is the effect of wind direction on (10). This uncertainty was estimated by determining the difference in the exponential term from using our calculated angle Θ and an angle corresponding to the full plume radius, the latter of which would result in no plume being observed by the TECO 14D/E oxides-of-nitrogen analyzer. The calculated difference in the exponential term is less than 10% on average. The uncertainty involved in the determination of plume radius using 1 min wind directions cannot be easily quantified. The plumes of largest calculated radius tend to indicate greater NO_x production results than the plumes of smaller calculated radius. This implies that the smaller radii may be underestimated. Other contributions to the uncertainty of Q_p include manufacturer's specified accuracies of ±5% for the NO_x analyzer and ±3% for the strip chart recorder. Using an rms procedure with the contributions above yields an uncertainty of ±13% for Q_p.

Acknowledgments. Support for data collection and analyses was provided by the U.S. Department of Energy, Office of Science, Office of Biological and Environmental Research, under contract W-31-109-ENG-38. We are especially grateful to William Jafferis, Manager of the NASA RTLP site at Kennedy Space Center, for providing facilities for the studies; to Tony Eckoff, Bradley Burns, and Stan Star of I-NET, Inc., for providing technical information about the HGV-8 lightning simulator; to Boeing Aerospace Corporation for providing the HGV-8 lightning simulator for the study; and to Joe Michael of the Chemistry Division of Argonne National Laboratory for information on NO_2 production reactions.

References

Baulch, D. L., D. D. Drysdale, D. G. Horne, and A. C. Lloyd, *Evaluated Kinetic Data for High Temperature Reactions*, vol. 2, *Homogeneous Gas Phase Reactions of the H_2-N_2-O_2 System*, Butterworths, London, 1973.

Bemand, P. P., M. A. A. Clyne, and R. T. Watson, Reactions of chlorine oxide radicals, part 4, Rate constants for the reactions Cl + OClO, O + OClO, H + OClO, NO + OClO and O + ClO, *J. Chem. Soc., Faraday Trans. I*, *69*, 1356–1374, 1973.

Borucki, W. J., and W. L. Chameides, Lightning: Estimates of the rates of energy dissipation and nitrogen fixation, *Rev. Geophys.*, *22*, 363–372, 1984.

Chameides, W. L., D. H. Stedman, R. R. Dickerson, D. W. Rusch, and R. J. Cicerone, NO_x production in lightning, *J. Atmos. Sci.*, *34*, 143–149, 1977.

Christian, H. J., et al., Global frequency and distribution of lightning as observed by the optical transient detector (OTD), in *Proceedings of the 11th International Conference on Atmospheric Electricity*, ICAE, pp. 726–729, Guntersville, Ala., 1999.

Ford, H. D., and N. Endow, Rate constants at low concentrations, III, Atomic energy reactions in the photolysis of NO_x at 3660 A, *J. Chem. Phys.*, *27*(5), 1156–1160, 1957.

Franzblau, E., and C. J. Popp, Nitrogen oxides produced from lightning, *J. Geophys. Res.*, *94*, 11,089–11,104, 1989.

Frenzen, P., and C. A. Vogel, The turbulent kinetic energy budget in the atmospheric surface layer: A review and an experimental reexamination in the field, *Boundary Layer Meteorol.*, *60*, 49–76, 1992.

Goldenbaum, G. C., and R. R. Dickerson, Nitric oxide production by lightning discharges, *J. Geophys. Res.*, *98*, 18333–18338, 1993.

Hanna, S. R., G. A. Briggs, and R. P. Hosker, *Handbook on Atmospheric Dispersion*, *DOE/TIC-11223*, U.S. Dep. of Energy Tech. Inf. Cent., Washington, D. C., 1982.

Hill, R. D., Lightning channel decay, *Physics of Fluids B*, *2*(12), 3209–3211, 1990.

Hill, R. D., R. G. Rinker, and H. D. Wilson, Atmospheric nitrogen fixation by lightning, *J. Atmos. Sci.*, *37*, 179–192, 1980.

Hill, R. D., I. Rahmin, and R. G. Rinker, Experimental study of the production of NO, N_2O, and O_3 in a simulated atmospheric corona, *I & EC Res.*, *27*, 1264–1269, 1988.

Holler, H., U. Finke, H. Huntrieser, M. Hagen, and C. Feigl, Lightning-produced NO_x (LINOX)—Experimental design and case study results, *J. Geophys. Res.*, *104*, 13,911–13,922, 1999.

Huntrieser, H., H. Schlager, C. Feigl, and H. Holler, Transport and production of NO_x in electrified thunderstorms: Survey of previous studies and new observations at midlatitudes, *J. Geophys. Res.*, *103*, 28,247–28,264, 1998.

Kaufman, F., N. J. Gerri, and R. E. Bowman, Role of nitric oxide in the thermal decomposition of nitrous oxide, *J. Chem. Phys.*, *25*(1), 106–115, 1956.

Kotaki, M., and C. Katoh, The global distribution of thunderstorm activity observed by the Ionospheric Sounding Satellite (ISS-b), *J. Atmos. Sol. Terr. Phys.*, *45*, 833–847, 1983.

Lawrence, M. G., W. L. Chameides, P. S. Kasibhatla, H. Levy, and W. Moxim, Lightning and atmospheric chemistry: The rate of atmospheric NO production, in *Handbook of Atmospheric Electrodynamics*, vol. 1, edited by H. Volland, pp. 189–202, CRC Press, Boca Raton, Fla., 1994.

Lee, D. S., I. Kohler, E. Grobler, F. Rohrer, R. Sausen, L. Gallardo-Klenner, J. G. J. Olivier, F. J. Dentener, and A. F. Bouwman, Estimations of global NO_x emissions and their uncertainties, *Atmos. Environ.*, *31*, 1735–1749, 1997.

Levine, J. S., R. S. Rogowski, G. L. Gregory, W. E. Howell, and J. Fishman, Simultaneous measurements of NO_x, NO, and O_3 production in a laboratory discharge: Atmospheric implications, *Geophys. Res. Lett.*, *8*, 357–360, 1981.

Levy, H., II, W. J. Moxim, and P. S. Kasibhatla, A global three-dimensional time-dependent lightning source of tropospheric NO_x, *J. Geophys. Res.*, *101*, 22,911–22,922, 1996.

Liaw, Y. P., D. L. Sisterson, and N. L. Miller, Comparison of field, laboratory, and theoretical estimates of global nitrogen fixation by lightning, *J. Geophys. Res.*, *95*, 22,489–22,494, 1990.

Mackerras, D., M. Darveniza, R. E. Orville, E. R. Williams, and S. J. Goodman, Global lightning: Total, cloud, and ground flash estimates, *J. Geophys. Res.*, *103*, 19,791–19,809, 1998.

Medelius, P., and A. Eckoff, Simulated lightning and measurement systems on the space shuttle payload changeout room, I-NET, Inc., Dec. 1993.

Michael, J. V., J. E. Allen Jr., and W. D. Brobst, Temperature dependence of the NO + O_3 reaction rate from 195° to 369°K, *J. Phys. Chem.*, *85*, 4109–4117, 1981.

Peyrous, R., and R.-M. Lapeyre, Gaseous products created by electrical discharges in the atmosphere and condensation nuclei resulting from gaseous phase reactions, *Atmos. Environ.*, *16*(5), 959–968, 1982.

Picone, J. M., J. P. Boris, J. R. Grieg, M. Raleigh, and R. F. Fernsler, Convective cooling of lightning channels, *J. Atmos. Sci.*, *38*, 2056–2062, 1981.

Plooster, M. N., Numerical model of the return stroke of the lightning discharge, *Phys. Fluids*, *14*, 2124–2133, 1971.

Price, C., J. Penner, and M. Prather, NO_x from Lightning, 1, Global distribution based on lightning physics, *J. Geophys. Res.*, *102*, 5929–5941, 1997.

Ridley, B. A., J. E. Dye, J. G. Walega, J. Zheng, F. E. Grahek, and W. Rison, On the production of active nitrogen by thunderstorms over New Mexico, *J. Geophys. Res.*, *101*, 20,985–21,005, 1996.

Tuck, A. F., Production of nitrogen oxides by lightning discharges, *Q. J. R. Meteorol. Soc.*, *102*, 749–755, 1976.

Turman, B. N., and B. C. Edgar, Global lightning distributions at dawn and dusk, *J. Geophys. Res.*, *87*, 1191–1206, 1982.

Uman, M., and R. E. Voshall, Time interval between lightning strokes and the initiation of dart leaders, *J. Geophys. Res.*, *73*, 497–506, 1968.

Wacker, R. S., and R. E. Orville, Changes in measured lightning flash count and return stroke peak current after the 1994 U.S. National Lightning Detection Network upgrade, 1, Observations, *J. Geophys. Res.*, *104*, 2151–2157, 1999.

Wang, Y., A. W. Desilva, G. C. Goldenbaum, and R. Dickerson, Nitric oxide production by simulated lightning: Dependence on current, energy and pressure, *J. Geophys. Res.*, *103*, 19,149–19,159, 1998.

Winn, W. P., G. W. Schwede, and C. B. Moore, Measurement of electric fields in thunderstorms, *J. Geophys. Res.*, *79*, 1761–1767, 1974.

Yarwood, G., J. W. Sutherland, M. A. Wickramaaratchi, and R. B. Klemm, Direct rate constant measurements for the reaction O + NO + Ar → NO_2 + Ar at 300–1341 K, *J. Phys. Chem.*, *95*, 8771–8775, 1991.

D. R. Cook, Y. P. Liaw, and D. L. Sisterson, Environmental Research Division, Argonne National Laboratory, 9700 S. Cass Avenue, Building 203, Argonne, IL 60439. (drcook@anl.gov)

N. L. Miller, Earth Sciences Division, Berkeley National Laboratory, University of California, One Cyclotron Road, M/S 90-1116, Berkeley, CA 94720.

(Received July 21, 1999; revised November 15, 1999; accepted November 18, 1999.)